Excitonic Nonlinearities of Semiconductor Microcavities in the Nonperturbative Regime

F. Jahnke, M. Kira, and S. W. Koch
Department of Physics and Material Sciences Center, Philipps-University, Marburg, Germany

G. Khitrova, E. K. Lindmark, T. R. Nelson, Jr., D. V. Wick, J. D. Berger, O. Lyngnes, and H. M. Gibbs
Optical Sciences Center, University of Arizona, Tucson, Arizona 85721

K. Tai
Institute of Electro-Optical Engineering, National Chiao Tung University, Hsinchu, Taiwan, Republic of China
(Received 2 July 1996)

A microscopic theory for excitonic nonlinearities and light propagation in semiconductor microcavities is applied to study normal-mode coupling (NMC) for varying electron-hole-pair densities. The nonlinear susceptibility of quantum confined excitons is determined from quantum kinetic equations including dephasing due to carrier-carrier and polarization scattering. The predicted disappearing of the normal-mode transmission peaks with negligible change in the NMC splitting agrees well with cw pump-probe measurements on samples showing remarkable splitting-to-linewidth ratios. [S0031-9007(96)01904-7]

PACS numbers: 71.35.Cc, 71.36.+c, 73.20.Dx

Atom-photon interaction in the strong-coupling regime is realized in high-finesse cavities where the coupling strength between the atom and the cavity mode exceeds both the cavity and atomic damping and the spontaneous emission rate. For the interaction of a *single excited atom* with an empty cavity in the strong coupling regime vacuum field Rabi oscillations have been predicted [1] and observed [2]. When the number of excited atoms is large compared to the number of cavity photons the quantum treatment of the system by means of master equations becomes equivalent to the semiclassical treatment of Maxwell-Bloch equations [3] and the resonance splitting can be assigned to the normal-mode coupling (NMC) of classical oscillators. Recently, NMC of quantum confined excitons in high-finesse semiconductor microcavities has been observed [4]. In contrast to experiments with preexcited atoms, the semiconductor excitons in the microcavity are coherently driven by the weak probe field. The coupled system of excitons and cavity field can be described in terms of new states similar to exciton polaritons. However, radiatively stable polaritons can exist only in bulk semiconductors whereas in quantum wells (QWs) the lack of momentum conservation in the growth direction leads to an intrinsic radiative lifetime [5,6]. Large cavity-polariton NMC splitting has been demonstrated in wide-gap II-VI semiconductor QW microcavities [7] and III-V semiconductor bulk microcavities [8] and NMC could even be observed at room temperature [9]. Recently, the nonlinear saturation of the NMC has been investigated experimentally [10,11].

In this Letter we study the microscopic mechanisms for nonlinear saturation of QW excitons and the corresponding modification of the NMC in a microcavity. We compare the influence of broadening and reduction of the oscillator strength and study the transition from the so-called strong-coupling to the weak-coupling regime. Theoretical results are compared with pump-probe measurements on samples with remarkably large splitting-to-linewidth ratios. It turns out that carrier-carrier and polarization scattering has to be considered in order to explain the experiments.

In most recent publications [12–14] the theoretical description of QW polaritons in semiconductor microcavities was based on a linear dispersion theory or phenomenological exciton Hamiltonians. The broadening of the excitons has been described as a constant parameter and the coupling between the 1*s* exciton and higher bound and continuum states has been neglected. However, earlier studies of bulk and QW excitons without microcavities have shown that exciton saturation is a microscopically intricate process. Additional unbound carriers, e.g., generated through an additional optical pulse resonant with the interband continuum, can efficiently bleach the exciton resonances. Phase-space filling and screening lead to a reduction of the exciton oscillator strength and binding energy as well as to band gap renormalization. Free carriers can scatter among each other and with the excitonic polarization. The corresponding dephasing leads to a broadening of the excitonic resonances.

Often, nonlinear saturation experiments with bulk or QW excitons cannot reveal whether bleaching of the excitonic resonances is due to a reduction of the oscillator strength or due to resonance broadening. As we will show, the strong coupling regime in microcavities can help to distinguish between both effects. The width of the NMC splitting depends only on the oscillator strength whereas the width of the NMC peaks is influenced by excitonic broadening.

Excitonic bound states in the presence of an electron-hole plasma have been treated in the past using a Bethe-Salpeter equation [15–17], whereas the coherent exciton

dynamics is described by semiconductor Bloch equations [18]. Only recently a microscopic analysis of excitonic broadening due to carrier-carrier interaction has been presented [19]. In this Letter, we use a kinetic equation for the coherent exciton polarization to study the saturation of the excitonic states and the corresponding saturation of the excitonic NMC. The kinetic equation describes coupled bound and continuum states of QW excitons under the influence of phase-space filling, screening, and dephasing due to additional unbound electron-hole pairs. Using the nonequilibrium Green's functions technique we obtain for the coherent interband polarization $\Psi_k(t)$ with the in-plane momentum k (for the lowest subband)

$$\left[i\hbar\frac{\partial}{\partial t} - \varepsilon_k^e - \varepsilon_k^h\right]\Psi_k(t) + [1 - f_k^e - f_k^h]\Omega_k(t) = -i\hbar\Gamma_k\Psi_k(t) + i\hbar\frac{1}{L^2}\sum_{k'}\Gamma_{k,k'}\Psi_{k'}(t). \quad (1)$$

The screened Hartree-Fock self-energies

$$\Omega_k(t) = d_k E(t) + \frac{1}{L^2}\sum_{k'} V^S_{k-k'}\Psi_{k'}(t), \quad (2)$$

$$\varepsilon_k^a = \epsilon_k^a + \frac{1}{L^2}\sum_{k'} V^S_{k-k'} f^a_{k'} + \frac{1}{2L^2}\sum_{k'}[V^S_{k'} - V_{k'}] \quad (3)$$

contain the free carrier energies $\epsilon_k^{e,h} = \frac{E_G}{2} + \frac{\hbar^2k^2}{2m_{e,h}}$ and the field $E(t)$ at the QW position which has to be computed self-consistently from Maxwell's equations.

We consider a weak external field that probes excitonic properties in the presence of distributions $f_k^{e,h}$ of unbound electrons and holes. For a sufficiently long time delay between the electron-hole-pair generation and the optical probe pulse, carrier-carrier and carrier-phonon scattering leads to a quasiequilibration of the carriers within their bands so that $f_k^{e,h}$ can be taken as Fermi-Dirac distributions. Phase-space filling due to these carriers is described by the $1 - f_k^e - f_k^h$ factor in Eq. (1) and the corresponding band gap shrinkage follows from Eq. (3). Carrier scattering leads to a rapid dephasing. In second Born approximation the corresponding diagonal damping rate, which is usually assumed to generalize the T_2 time for two-level systems, is given by

$$\Gamma_k = \frac{\pi}{\hbar}\sum_{a,b=e,h}\frac{1}{L^4}\sum_{k_1,k_2}\delta[\epsilon_k^a + \epsilon^b_{k_1+k_2-k} - \epsilon^b_{k_2} - \epsilon^a_{k_1}][2(V^S_{k-k_1})^2 - \delta_{a,b}V^S_{k-k_1}V^S_{k-k_2}] \times [(1 - f^b_{k_1+k_2-k})f^b_{k_2}f^a_{k_1} + f^b_{k_1+k_2-k}(1 - f^b_{k_2})(1 - f^a_{k_1})]. \quad (4)$$

In Eq. (4) the term $\propto 2(V^S_{k-k_1})^2$ describes the direct or RPA contribution whereas the term $\propto \delta_{a,b}V^S_{k-k_1}V^S_{k-k_2}$ is the exchange contribution (vertex correction). The δ function in Eq. (4) accounts for energy conservation during the scattering process (in Markov approximation) and the occupation probabilities f describe the availability of initial and final states. Interaction between carriers and the coherently driven interband polarization also leads to nondiagonal contributions

$$\Gamma_{k,k_1} = \frac{\pi}{\hbar}\sum_{a,b=e,h}\frac{1}{L^2}\sum_{k_2}\delta[\epsilon_k^a + \epsilon^b_{k_1+k_2-k} - \epsilon^b_{k_2} - \epsilon^a_{k_1}][2(V^S_{k-k_1})^2 - \delta_{a,b}V^S_{k-k_1}V^S_{k-k_2}] \times \{[1 - f_k^a](1 - f^b_{k_1+k_2-k})f^b_{k_2} + f_k^a f^b_{k_1+k_2-k}(1 - f^b_{k_2})\}. \quad (5)$$

The macroscopic polarization entering Maxwell's equations is given by $P(t) = \frac{1}{L^2}\sum_k d_k\Psi_k(t)$ and the excitonic susceptibility $\chi(\omega) = P(\omega)/E(\omega)$ contains the Fourier transform of $P(t)$ and $E(t)$.

In a first step we solve Eqs. (1)–(5) to study the saturation of the excitonic susceptibility for a given plasma density. Screening is described within a quasistatic single plasmon-pole approximation. The solid line in Fig. 1(a) shows the computed exciton spectrum where all terms of Eqs. (4) and (5) have been considered. The broadening increases by almost a factor of 2 when the exchange contributions in Eqs. (4) and (5) are neglected (dashed line). In the pure dephasing limit, where only diagonal dephasing due to carrier-carrier scattering according to Eq. (4) is considered, the broadening is strongly overestimated (dotted line). Off-diagonal dephasing compensates diagonal dephasing to a large extent. Somewhat similar behavior has been found for resonant interband excitation where the generation process of free carriers is accurately described only if diagonal and off-diagonal dephasing contributions are considered [20].

In Fig. 1(b) a full calculation is compared with the case of constant damping. For the microscopic model the broadening of various bound states is different and the low energy tail of the 1s exciton decreases faster than the Lorentzian tail for constant damping. For a higher carrier density (10^{11} cm^{-2}) we obtain with constant damping and static screening the well-known artificial shift of the 1s exciton whereas the full dephasing calculation does not exhibit this shift. For the higher carrier density and the same constant damping the height of the 1s exciton peak is reduced by a factor of only about 2.5 due to phase-space filling and screening. If the increased broadening is also taken into account within the full calculation, the height of the 1s exciton peak is reduced almost by an order of magnitude. Figure 2(a) shows the saturation of the 1s exciton for increasing plasma density computed within the full dephasing model.

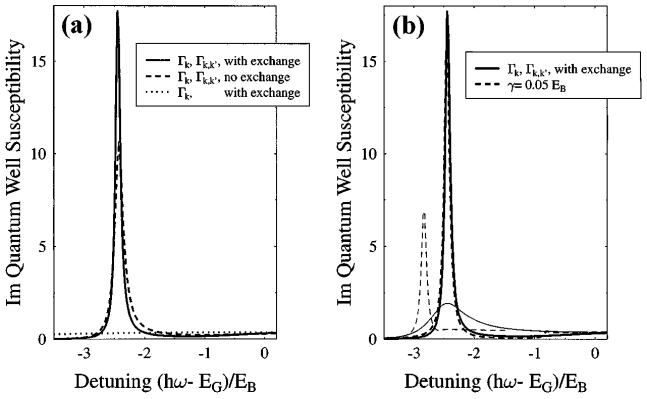

FIG. 1. (a) Imaginary part of the optical susceptibility for an 8 nm QW and plasma excitation with 10^{10} cm^{-2} at 77 K with full dephasing (solid line), without exchange interaction (dashed line) and without nondiagonal polarization scattering (dotted line). (b) Comparison of full dephasing (solid line) and constant damping (dashed line). The carrier densities are 10^{10} cm^{-2} (thick lines) and 10^{11} cm^{-2} (thin lines).

To calculate the NMC spectrum for the QW inside the microcavity one additionally has to solve Maxwell's equations for the full resonator structure. For an incoming light beam at normal incidence to the Bragg mirrors the wave equation can be written as

$$\left[\frac{\partial^2}{\partial z^2} + \frac{\omega^2}{c_0^2} n^2(z)\right] E(z,\omega) = -\mu_0 \omega^2 \chi(\omega)\,|\xi(z)|^2 \times \int dz' |\xi(z')|^2 E(z',\omega)\,. \tag{6}$$

$n(z)$ describes the index profile across the microresonator. The z dependence of the macroscopic polarization, which is expressed in Eq. (6) by the susceptibility χ, is given by confinement functions $|\xi(z)|^2$. The self-consistently determined field component at the QW position, $\int dz' |\xi(z')|^2 E(z')$, also enters the calculation of the QW polarization.

We evaluate the coupled equations for a $\frac{3}{2}\lambda$ cavity with two QWs at the field antinodes. For the top mirror (exposed to air) and bottom mirror (on a substrate) a reflectivity of 99.6% is obtained with 14 and 16.5 quarter-wave pairs. The cavity wavelength is chosen to coincide with the 1s exciton resonance of the QWs. The calculated microcavity transmission is shown in Fig. 2(b). For increasing bleaching of the 1s exciton resonance with increasing carrier density we find a strong reduction of the NMC peak height with only a small reduction of the NMC splitting. The increasing width of the individual NMC peaks indicates the strong broadening of the exciton resonance, whereas the small reduction of the splitting clearly reveals the minor reduction of the exciton oscillator strength within a large plasma density range. With increasing plasma density the renormalized band edge approaches the energetically stable-1s-exiton resonance. The rather abrupt

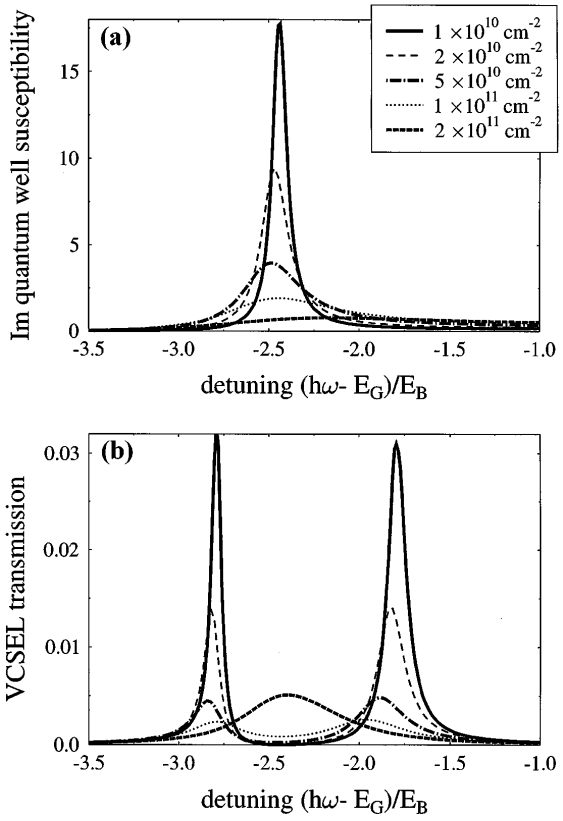

FIG. 2. (a) Imaginary part of the optical susceptibility for an 8 nm QW and plasma excitation with various densities at carrier temperature 77 K. (b) Calculated transmission of the QW microcavity for increasing plasma density and bleaching of the exciton according to Fig. 2(a). The cavity resonance has been tuned from -2.05 (full line) to -2.14 (short dashed line) to compensate for the small numerical exciton shift.

replacement of the normal mode doublet by a single transmission peak occurs when the cavity resonance becomes degenerate with the band edge. This corresponds to the transition from the strong-coupling regime to the weak-coupling regime, since the damping of the continuum states strongly exceeds the dipole coupling.

Our theoretical results for the nonlinear NMC saturation are consistent with measurements. In Refs. [10,11] nonlinear data are presented in the regime of reduced oscillator strength, but the broad linewidths prevented the observation of exciton broadening with little reduction of the splitting. We clearly observe this effect in experiments with 8 nm $In_{0.04}Ga_{0.96}As$ QWs between thick GaAs barriers within GaAs/AlAs Bragg mirrors. The In concentration is sufficiently large for the heavy-hole exciton peak to be around 834 nm at 4 K, so that the GaAs substrate does not have to be removed for transmission studies. Nonetheless the strain shifts the light-hole exciton peak to 826 nm, so that it does not interfere with NMC studies with the heavy hole. The small exciton linewidth (1 meV = 0.6 nm at 4 K) leads to record splitting-to-linewidth ratios of 6.8 for Bragg mirrors consisting of

14 and 16.5 periods for the top and bottom mirrors, respectively, with 99.6% calculated reflectivity.

We have performed cw pump-probe measurements of the exciton saturation and the nonlinear transmission of a microcavity exhibiting NMC. A light-emitting diode with peak wavelength at 850 nm and a spectral FWHM of 50 nm is used as a broadband probe; it is square wave modulated at 6 kHz and detected with an R636 photomultiplier tube and lock-in amplifier. The pump beam from a Ti:sapphire laser is focused on the microcavity to 46 μm diameter, sufficiently larger than the 30 μm probe diameter. Figure 3(a) shows that as the exciton is saturated by band-to-band pumping, at first there is little change in oscillator strength (integrated absorption) but considerable broadening [21]. This broadening increases the absorption at the wavelengths of the two peaks thereby decreasing their transmission as shown in Fig. 3(b). When the exciton is completely saturated, the transmission of the almost-empty cavity opens up close to the midpoint (the usual weak-coupling laser limit). Figure 3(b) was taken with the pump wavelength at the first transmission minimum above the stopband. The same reduction in transmission without reduction in splitting is seen when the pump wavelength is coincident with either of the original peaks or midway between them; of course, the power dependence is different for each of the wavelengths.

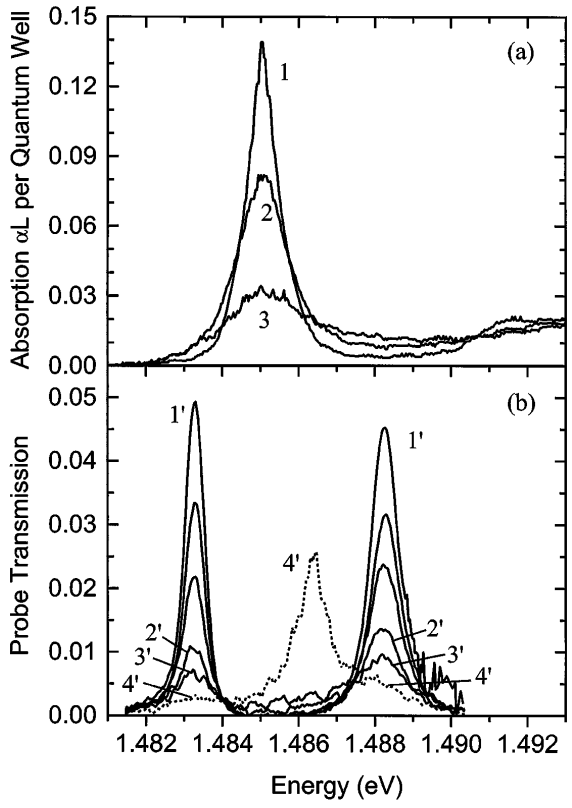

FIG. 3. Experimental probe transmission spectra with increasing pumping at 787 nm for (a) exciton absorption of 20 QWs like the two in the microcavity and (b) microcavity NMC. Since absolute densities are not measured, curves in (a) and (b) cannot be compared directly; however, Kramers-Kronig transfer-matrix microcavity calculations using the nonlinear data in (a) show that $2'$ corresponds closely to 2 and $3'$ to 3. Noise from photoluminescence prevented determining the probe transmission when the exciton is completely saturated corresponding to $4'$. Stronger pumping in (b) results in lasing at a wavelength close to the $4'$ peak. The 20-QW data in (a) were shifted by 4 meV to the position of the 2-QW peak in the NMC microcavity as deduced from the data of (b).

In conclusion we have studied the nonlinear saturation of the excitonic NMC in QW microcavities. With increasing carrier density we find a strong broadening of the excitonic states without significant loss of oscillator strength. For carrier densities leading to exciton saturation we observe the transition from the strong coupling regime with periodic energy exchange between the cavity-like and excitonic states to the weak coupling regime of cavity enhanced emission.

The Marburg group acknowledges a grant for CPU time at the Forschungszentrum Jülich. Support from AFOSR, NSF, ARPA/ARO, JSOP, and COEDIP is acknowledged from the Tucson group.

[1] J. J. Sanchez-Mondragon, N. B. Narozhny, and J. H. Eberly, Phys. Rev. Lett. **51**, 550 (1983).
[2] R. J. Thompson, G. Rempe, and H. J. Kimble, Phys. Rev. Lett. **68**, 1132 (1992).
[3] Y. Zhu *et al.*, Phys. Rev. Lett. **64**, 2499 (1990).
[4] C. Weisbuch, M. Nishioka, A. Ishikawa, and Y. Arakawa, Phys. Rev. Lett. **69**, 3314 (1992).
[5] V. M. Agranovich and O. A. Dubovskii, JETP Lett. **3**, 223 (1966).
[6] E. Hanamura, Phys. Rev. B **38**, 1228 (1988).
[7] P. Kelkar *et al.*, Phys. Rev. B **52**, 5491 (1995).
[8] A. Tredicucci *et al.*, Phys. Rev. Lett. **75**, 3906 (1995).
[9] R. Houdré *et al.*, Phys. Rev. B **49**, 16 761 (1994).
[10] R. Houdré *et al.*, Phys. Rev. B **52**, 7810 (1995).
[11] J.-K. Rhee *et al.*, Solid State Commun. **97**, 941 (1996).
[12] D. S. Citrin, IEEE J. Quantum Electron. **30**, 997 (1994).
[13] V. Savona, L. C. Andreani, P. Schwendimann, and A. Quattropani, Solid State Commun. **93**, 733 (1995).
[14] S. Jorda, Phys. Rev. B **50**, 18 690 (1994).
[15] R. Zimmermann *et al.*, Phys. Status Solidi (b) **90**, 175 (1978).
[16] H. Haug and S. Schmitt-Rink, J. Opt. Soc. Am. B **2**, 1135 (1985).
[17] W. Schäfer, R. Binder, and K. H. Schuldt, Z. Phys. B **70**, 145 (1988).
[18] See, e.g., H. Haug and S. W. Koch, *Quantum Theory of the Optical and Electronic Properties of Semiconductors* (World Scientific Publ., Singapore, 1994), 3rd ed.
[19] W. Schäfer, J. Opt. Soc. Am. B (to be published).
[20] F. Rossi, S. Haas, and T. Kuhn, Phys. Rev. Lett. **72**, 152 (1994).
[21] The nonlinear behavior here is different from Refs. [10, 11] because the inhomogeneous broadening here is much smaller than the NMC splitting so that the homogeneous broadening can have such a dramatic effect on the two transmission peaks before loss of oscillator strength.